

## DEM AND TFM SIMULATIONS OF SOLIDS MIXING IN A GAS-SOLID FLUIDIZED BED

Willem GODLIEB, Sander GORTER, Niels G. DEEN\* and J.A.M. KUIPERS

University of Twente, Institute for Mechanics Processes and Control Twente (IMPACT),  
 Faculty of Science and Technology, PO Box 217, NL-7500 AE Enschede, THE NETHERLANDS,  
 and Dutch Polymer Institute, PO Box 902, 5600 AX Eindhoven, THE NETHERLANDS

\*Corresponding author, E-mail address: N.G.Deen@utwente.nl

### ABSTRACT

In the production and processing of granular matter, mixing of solids plays an important role. Granular materials such as sand, polymeric particles and fertilizers are processed in different apparatus such as fluidized beds, rotary kilns and spouted beds. In the operation of these apparatus proper mixing is essential, as it helps to prevent formation of hot-spots, off-spec products and undesired agglomerates. DEM can be used to simulate these granular systems in detail and provide insight in mixing phenomena. Several methods to analyse and characterize mixing on basis of DEM data have been proposed in the past, but there is no general consensus on what method to use.

In this paper we discuss various methods that are available to give quantitative information on the solids mixing state in granular systems based on DEM and TFM simulations. We apply the different methods to full 3D DEM simulations of a fluidized bed and to tracer particles in full 2D TFM simulations. It is found that some of these methods are grid dependent, are not reproducible, are sensitive to macroscopic flow patterns and/or are only able to calculate overall mixing indices, rather than indices for each direction. We compare some methods described in literature and in addition propose two new methods, which do not suffer from the disadvantages mentioned above.

Simulations are performed for seven different operating pressures. It is found that mixing improves with operating pressure caused by increased porosity and increased granular temperature of the particulate phase.

### NOMENCLATURE

$A$	Amplitude (-)
$d$	Diameter (m)
$D$	Discrete Dirac delta function (-)
$\Delta t$	Time step (s)
$F$	Force ( $\text{kg m s}^{-2}$ )
$g$	Gravitational acceleration ( $\text{m s}^{-2}$ )
$m$	Mass (kg)
$M$	Mixing index (-)
$N$	Number of particles (-)
$p$	Pressure ( $\text{N m}^{-2}$ )
$r_{ij}$	Distance between two particles (m)
$r_p$	particle radius
$S^2$	Variance (-)
$\bar{S}_p$	Sink term ( $\text{kg m}^2 \text{s}^{-1}$ )
$t$	Time (s)
$u$	Gas velocity ( $\text{m s}^{-1}$ )

$v$	Solids velocity ( $\text{m s}^{-1}$ )
$V$	Volume ( $\text{m}^3$ )
$x$	X-coordinate (m)
$y$	Y-coordinate (m)
$z$	Z-coordinate (m)

### Greek letters

$\beta$	Momentum transfer coefficient ( $\text{kg s}^{-1} \text{m}^{-2}$ )
$\delta$	Dimensionless distance (-)
$\varepsilon$	Porosity (-)
$\phi$	Particle concentration (-)
$\gamma$	Damping coefficient ( $\text{s}^{-1}$ )
$\mu$	Viscosity ( $\text{kg m}^{-1} \text{s}^{-1}$ )
$\rho$	Density ( $\text{kg m}^{-3}$ )
$\bar{\tau}_f$	Gas phase stress tensor ( $\text{kg m}^2 \text{s}^{-1}$ )
$\theta$	Granular temperature ( $\text{m}^2 \text{s}^{-2}$ )
$\omega$	Period ( $\text{rad s}^{-1}$ )

### Subscripts

diff	different
f	fluid
fit	fitted
g	gas
i,j,k,m	particle numbers
M	mean
mf	minimum fluidization
n	normal
sup	superficial
t	tangential

### INTRODUCTION

Gas fluidized beds are widely used in industry in various large-scale processes involving physical and/or chemical operations. The large specific surface area of the solids in fluidized beds is beneficial for various operations, such as gas-solid reactions, cooling and drying. In many cases it is important that all particles are well mixed so that all particles cool, react or dry in a similar manner, to prevent hot spot formation or agglomeration.

Solids mixing of granular materials is researched widely. Since solids mixing is difficult to characterize experimentally, some groups use discrete element models (DEM) or discrete particle models (DPM) to investigate solids mixing behaviour. McCarthy et al. (2000) succeeded to validate their simulations with experiments, which indicates that modelling is a promising approach to describe solids mixing in detail.

In this work we investigate the capabilities of four different methods that can be used to calculate a mixing

index from DPM simulations and two-fluid model (TFM) simulations of fluidized beds. A mixing index (M) is used to quantify the state of mixedness of the system and is zero or one for respectively fully demixed and fully mixed conditions. The mixing index is also known as entropy of mixing (Schutyser et al., 2001), whereas Lu and Hsiau (2005) call it mixing degree, and Finnie et al. (2005), Asmar et al (2002) and Van Puyvelde (2006) call it mixing index. While most authors try to determine the mixing index from DEM simulations, they use different methods: Schutyser et al. (2001) calculated entropy based on entropy equations from molecular dynamics, whereas Mostoufi and Chaouki (2001) used the "colour" of a marked region (a spot) in the middle of the bed and measured the radius of the spot as a function of time. They were not able to calculate a mixing index. Lu and Hsiau (2005) and Rhodes et al. (2001) use the Lacey index as mixing index, which will be described later.

Two-fluid models or Euler-Euler models use the kinetic theory of granular flow (KTGF) for the particulate phase. With these models mixing can be determined with stating two particulate phases as shown by Darelius et al. (2008). In this work we use tracer particles that move with the interpolated velocity of the particulate phase. By using tracer particles, the same methods used for analysing DPM results can be used to analyse mixing from TFM simulation data.

We test two new methods to quantify mixing: one based on the colouring of the twelve nearest neighbours and a method based on the increasing distance of initially neighbouring particles. In this work we use the average height method and Lacey's method, as well as the two newly proposed methods to investigate solids mixing in a fluidized bed containing mono-disperse polymeric particles at different operating pressures. In the first part of this paper the governing equations of the DPM and TFM are presented, followed by the various methods to characterize solids mixing. Subsequently the results of the different methods applied to the simulation data are discussed and conclusions are presented.

## MODEL DESCRIPTION

### Discrete particle model

The discrete particle model (DPM) used in this work is an Euler-Lagrange model that was originally developed by Hoomans et al. (1996). In the DPM every particle is individually tracked accounting for particle-particle and particle-wall collisions. In the DPM the gas phase hydrodynamics is described by the Navier-Stokes equations:

$$\frac{\partial}{\partial t}(\varepsilon_f \rho_f) + (\nabla \cdot \varepsilon_f \rho_f \bar{u}) = 0 \quad (1)$$

$$\frac{\partial}{\partial t}(\varepsilon_f \rho_f \bar{u}) + (\nabla \cdot \varepsilon_f \rho_f \bar{u} \bar{u}) = -\varepsilon_f \nabla p - (\nabla \cdot \varepsilon_f \bar{\tau}_f) - \bar{S}_p + \varepsilon_f \rho_f \bar{g} \quad (2)$$

where  $\bar{u}$  is the gas velocity and  $\bar{\tau}_f$  represents the gas phase stress tensor. The sink term  $\bar{S}_p$ , represents the drag force exerted on the particles:

$$\bar{S}_p = \frac{1}{V_{cell}} \int_{V_{cell}} \sum_{i=0}^{N_p} \frac{V_i \beta}{\varepsilon_s} (\bar{u} - \bar{v}) D(\bar{x} - \bar{x}_i) dV \quad (3)$$

The distribution function  $D(\bar{x} - \bar{x}_i)$  is a discrete representation of a Dirac delta function that distributes the reaction force acting on the gas phase to the Eulerian grid via a volume-weighting technique. The inter-phase momentum transfer coefficient,  $\beta$  describes the drag of the gas-phase acting on the particles, which is modelled with the relation proposed by van der Hoef et al. (2005):

$$\beta = 18 \frac{\mu_f}{d^2} \left( 10 \frac{\varepsilon_s^2}{\varepsilon_f} + \varepsilon_f^3 \varepsilon_s (1 + 1.5 \sqrt{\varepsilon_s}) \right) \quad (4)$$

The motion of every individual particle  $i$  in the system is calculated from Newton's second law:

$$m_i \frac{d\bar{v}_i}{dt} = -V_i \nabla p + \frac{V_i \beta}{\varepsilon_s} (\bar{u} - \bar{v}_i) + m_i \bar{g} + \bar{F}_i^{pp} + \bar{F}_i^{pw} \quad (5)$$

where the forces on the right hand side are, respectively due to pressure, drag, gravity, particle-particle interaction and particle-wall interaction. The contact forces are caused by collisions with other particles or confining walls. These collisions are described with a soft-sphere approach. This approach uses a linear spring/dash-pot model, wherein the velocities, positions and collision forces of the particles are calculated at every fixed time step via a first order time integration. The collision model takes restitution and friction effects into account. The associated collision coefficients were obtained experimentally via the method of Kharaz et al. (1999). For more details on the implementation of the soft-sphere model we refer to the work of van der Hoef et al. (2006).

### Two-fluid model

In the two-fluid model (TFM) both the gas and solids phase are described as continuous inter-penetrating fluids. With the TFM, much larger simulate systems can be simulated, compared to the DPM. The equations of motion of the gas phase are the same as in the DPM (i.e. Eqs. (1) and (2)). In the TFM the interfacial momentum transfer is modelled by:

$$\bar{S}_p = \beta (\bar{u} - \bar{v}) \quad (6)$$

The motion of the solids phase is described by:

$$\frac{\partial}{\partial t}(\varepsilon_s \rho_s) + (\nabla \cdot \varepsilon_s \rho_s \bar{v}) = 0 \quad (7)$$

$$\frac{\partial}{\partial t}(\varepsilon_s \rho_s \bar{v}) + (\nabla \cdot \varepsilon_s \rho_s \bar{v} \bar{v}) = -\varepsilon_s \nabla p - (\nabla \cdot \varepsilon_s \bar{\tau}_s) - \nabla p_s + \bar{S}_p + \varepsilon_s \rho_s \bar{g} \quad (8)$$

For the equation of state of the solids phase the kinetic theory of granular flow (KTGF) is used. In addition to the continuity and the Navier-Stokes equations the granular temperature equation is solved for the particulate phase. The overall granular temperature is defined as:

$$\Theta = \frac{1}{3} \langle \bar{C}_p \cdot \bar{C}_p \rangle \quad (9)$$

where:

$$\bar{C}_p = \bar{c}_p - \bar{v} \quad (10)$$

Note that the particle velocity ( $\bar{c}_p$ ) is decomposed in the local mean velocity ( $\bar{v}$ ) and the fluctuation velocity component ( $\bar{C}_p$ ).

The granular temperature is given by:

$$\frac{3}{2} \left[ \frac{\partial}{\partial t}(\varepsilon_s \rho_s \Theta) + (\nabla \cdot \varepsilon_s \rho_s \Theta \bar{v}) \right] = -(\bar{p}_s \bar{I} + \varepsilon_s \bar{\tau}_s) : \nabla \bar{v} - \nabla \cdot (\varepsilon_s q_s) - 3\beta \Theta - \gamma \quad (11)$$

For a detailed description of all the used KTGF closure equations we refer to the work of Goldschmidt et al. (2001).

### Tracer particles

To investigate mixing in the TFM one could define multiple solids phases with the same properties, but different colours. Drawbacks of this approach are grid dependency, initial colouring dependency and the inability to investigate sub grid mixing. An attractive alternative to the use of multiple solids phases is the use of tracer particles. As the motion of the solids phase is visualized by tracer particles, the same methods for characterizing mixing as used in the DPM can be applied.

By definition tracer particles have no mass and follow the solids phase velocity exactly. The velocity of the tracer particles is interpolated from the solids phase velocity as follows:

$$\bar{v}_p = D(\bar{x} - \bar{x}_m)\bar{v}_s \quad (12)$$

In this work we use volume-weighting (i.e. tri-linear interpolation) for the interpolation:

$$D(\bar{x} - \bar{x}_m) = \prod_i D(x_i - x_{m,i}) \quad (13)$$

where

$$D(x_i - x_{m,i}) = \begin{cases} 1 - \delta_i & \text{if } \delta_i \leq 1; \\ 0 & \text{if } \delta_i > 1; \end{cases} \quad (14)$$

and

$$\delta_i = \frac{|x_i - x_{m,i}|}{\Delta x_i} \quad (15)$$

where  $\delta_i$  is the dimensionless distance between the Eulerian position  $x_i$  and the Lagrangian position of the marker  $x_{m,i}$  in the  $x_i$  direction.

## METHODS FOR CHARACTERIZING MIXING

In this work we use four different methods to obtain mixing indices from DPM data with mono-disperse particles. Each of these methods will now briefly be introduced.

### Average height method

The average height method is the simplest of the investigated methods and is based on the average height of a group of coloured particles. It is widely used for measuring segregation, for example by Hoomans et al. (2000). In the case of mono-disperse systems, half of the particles are given a colour, while all physical properties remain unchanged and are constant throughout the set of particles. Subsequently the average position of all particles is monitored. While the mixing behaviour can in principle be investigated in all three directions, here we will only explain mixing in the vertical direction. In the first step of the algorithm the vertical positions of all particles are sorted to determine the median height. Subsequently the lower half of the particles is coloured white, while the upper half is coloured black. For each time step the average height of the white particles can be calculated and normalized with the average height of all particles:

$$\bar{z}_{white} = \frac{\frac{1}{N_{white}} \sum_{i \in white} z_i}{\frac{1}{N_{all}} \sum_{i \in all} z_i} \quad (16)$$

where  $\bar{z}_{white}$  is the normalized average vertical position of the white particles. Notice that initially  $\bar{z}_{white} = 0.5$  and when the system fully mixed it becomes 1.0. We now define the mixing index as follows:

$$M = 2(\bar{z}_{white} - 0.5) \quad (17)$$

which means that for  $M = 0$  the system is fully demixed and for  $M = 1$  the bed is fully mixed.

This method can also be used to study lateral mixing. In those cases the left and right or front and back parts, are respectively coloured white and black.

### Lacey's method

The Lacey index is based on statistical analysis and was developed by Lacey (1954). The variance  $S^2$  for the concentration of the black particles in each cell is defined as follows:

$$S^2 = \frac{1}{N-1} \sum_{i=1}^N (\phi_i - \phi_m)^2 \quad (18)$$

where  $N$  is the number of cells in the bed containing particles and  $\phi_i$  the concentration of black particles in cell  $i$  and  $\phi_m$  the average concentration of black particles in the bed.

$S_0^2$  and  $S_R^2$  are defined as:

$$S_0^2 = \phi_m(1 - \phi_m) \quad (19)$$

$$S_R^2 = \frac{\phi_m(1 - \phi_m)}{n} \quad (20)$$

and respectively represent the variance of the unmixed bed and fully mixed bed.  $n$  is the average number of particles per cell.

The mixing index can be calculated as follows:

$$M = \frac{S^2 - S_0^2}{S_R^2 - S_0^2} \quad (21)$$

Due to the use of grid cells the Lacey index is grid dependent. A coarse grid gives higher mixing indices, since in that case micro mixing effects are neglected. A fine grid gives lower mixing indices, if only few particles are present in a cell. If only one particle is present in a cell it is always fully unmixed.

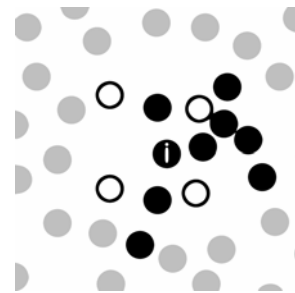


**Figure 1:** Illustration of the nearest neighbours method. For the highlighted particle ( $i$ ) the twelve nearest neighbours are shown. Four of them are white and eight are coloured black. Particles that are located further away are coloured grey and are not taken into account for this particle.

### Nearest neighbours method

Contrary to the average height method in which the overall average height of the particles is monitored, in the nearest neighbour method we evaluate the mixing in the vicinity of individual particles. Opposite to the Lacey index, it is grid independent. Initially we colour half of the

particles black, similar to what is done in the average height method. For each particle we determine the twelve nearest neighbouring particles. If these particles have the same colour as the particle under investigation it is unmixed, while if half of the nearest neighbours is coloured differently, it is fully mixed. This is expressed as follows:

$$M = \frac{1}{N_{part}} \sum_{N_{part}} \frac{2n_{diff}}{n_{nb}} \quad (22)$$

where  $n_{diff}$  is the number of nearest neighbours coloured differently and  $n_{nb}$  the number of nearest neighbours.

Figure 1 shows an example for one individual particle, for which four neighbouring particles have a different colour (i.e. white). The mixing index for particle  $i$  is  $2 \cdot 4 / 12 = 0.67$ . The overall mixing index is the average over all particles.

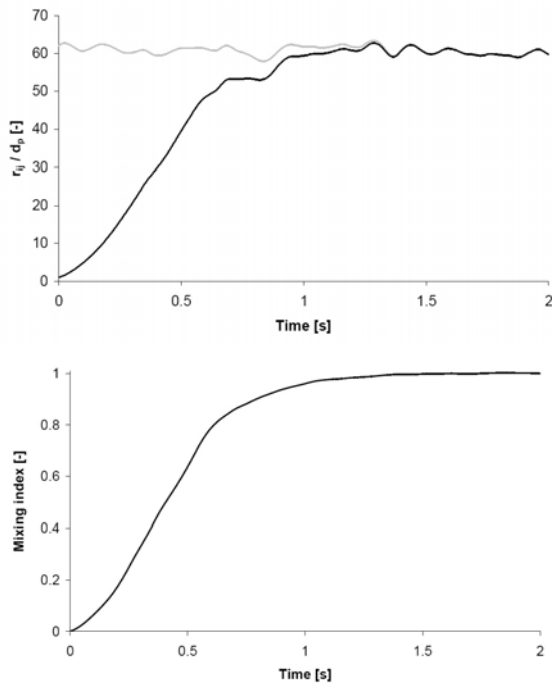


**Figure 2:** Top: Distance between initially nearest neighbours averaged over all pairs (black line) and average distance between random particles (grey line). Bottom: corresponding mixing index determined with the neighbour distance method.

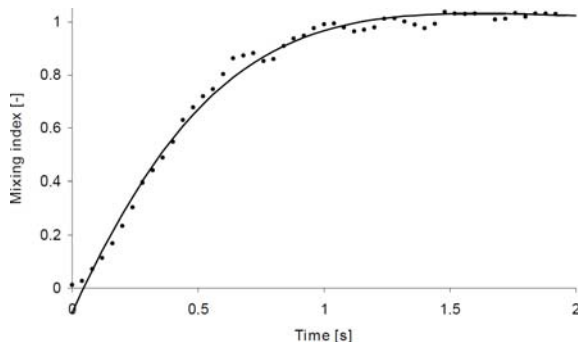


**Figure 3:** Lacey index fitted with a damped exponential function.

### Neighbour distance method

The fourth method used in this work is based on the distance between initial neighbours. At a given time the nearest neighbour is detected for each particle. Each particle and its nearest neighbour form a pair, and its centre to centre distance is monitored as time progresses. Initially the distance is in the order of one particle diameter and if the bed is fully mixed it can increase up to the bed dimensions.

Figure 2 (top) shows the average distance between initial neighbours normalized with the particle diameter. Initially it is just above one particle diameter and after 1 second it has increased up to 60 times the particle diameter. It is not a smooth curve, because bubbles let the bed expand and collapse, causing the distance between particles to increase and decrease with time. This effect introduces noise in the mixing measurement. Therefore the distance is normalised with the distance of randomly selected particle pairs (grey line), resulting in a smooth mixing curve, unaffected by bed expansions as seen in Figure 2 (bottom). Since initially the distance between neighbours is one particle diameter this is set to a mixing index of 0. The mixing index is expressed in the following equation:

$$M = \frac{\sum_{N_{part}} r_{ij} - d_p}{\sum_{N_{part}} r_{ik} - d_p} \quad (23)$$

where  $r_{ij}$  is the distance between particle  $i$  and its initially nearest neighbour  $j$  and  $r_{ik}$  is the distance between particle  $i$  and a randomly selected particle  $k$ .

The method just described can be used to calculate the mixing index for each direction. Note that in that case, initially the distance between the partners *in one direction* can be less than a particle diameter. Some basic algebra shows that the average distance in one direction for two touching particles is  $d_0 = 4d_p / \pi^2$ .

The mixing index in the vertical direction for the neighbour distance method is thus defined by:

$$M_z = \frac{\sum_{N_{part}} r_{ij,z} - d_0}{\sum_{N_{part}} r_{ik,z} - d_0} \quad (24)$$

The mixing index for the horizontal direction  $x$  or  $y$  can be obtained by replacing subscript  $z$  by  $x$  or  $y$  respectively.

### Calculation of the mixing time

The mixing index is a valuable quantity to investigate the solids mixing process in fluidized beds. To compare different simulations in a simple way, the mixing index curve is condensed in a single value. We choose to use the 95% mixing time  $t_{95\%}$ , where the mixing index reaches a value of 0.95. To prevent noise to influence the results, we fit a damped exponential function to the mixing index curve as follows:

$$M_{fit} = 1 - Ae^{-\lambda t} \quad (25)$$

where  $A$  and  $\lambda$ , are the amplitude and the damping coefficient respectively. Each of these coefficients is obtained from the simulation data using a least squares method. The fit as shown in Figure 3 accurately follows the trend of the curve. From this fit we can calculate the mixing time at which the bed is 95% mixed, by solving eq. 16 for  $t$ :

$$t_{95\%} = \frac{-1}{\lambda} \ln \left( \frac{1-0.95}{A} \right) \quad (26)$$

Unfortunately the average height method shows periodic overshoots. This effect is caused by the macroscopic circulation patterns of the particles in the bed, as can be seen in Figure 4, which shows the mixing index obtained for the average height method. Although  $M=1$  at 0.17 seconds the bed is not fully mixed. At 0.31 seconds the colour pattern has been more or less inverted due to the bed circulation patterns, leading to an overshoot of  $M=1.6$ . After about 1.8 seconds the overshoots have dampened out and the bed is almost entirely mixed. Since the mixing index is oscillating around a value of 1, it is hard to determine a mixing time; therefore the curve is fitted with a damped harmonic oscillator:

$$M_{fit} = 1 - Ae^{-\lambda t} \cos(\omega t) \quad (27)$$

where  $\omega$  is the period of the oscillation. Now we can calculate the 95% mixing time using the fit without the oscillator. By removing the periodic part from the fitted equation we obtain an expression similar to Eq. (25) from which a 95% mixing time can straightforwardly be obtained.

## RESULTS

2D TFM simulations of a pressurized bubbling fluidized bed at a constant excess velocity (i.e. superficial velocity minus the minimum fluidisation velocity) of 0.177 m/s were performed. The minimum fluidisation velocity was calculated with the Ergun equation. The mixing behaviour was analysed for operating pressures ranging from 1 bar to 64 bar, similar to the DPM simulations performed earlier by Godlieb et al. (2007a,b). The bed has dimensions of  $D = 0.025$  m and  $H = 0.15$  m and is filled with polymeric particles up to a static bed height of  $H_0 = 0.025$  m. The particles have a diameter of  $d_p = 1$  mm and a density of  $\rho_s = 925$  kg/m<sup>3</sup>. A computational stencil of 20 x 120 computational cells and a time step of  $2 \cdot 10^{-5}$  s was used. No-slip boundary conditions were used at the walls.

Unfortunately, the Lacey index mixing time could not be calculated for 64 bar, since the bed expanded too much so that there were not sufficient particles per cell and the Lacey index did not converge to 1 anymore.

The results of the vertical and horizontal mixing times are shown in Figure 5. It is found that the obtained trends show great similarities with the DPM results found by Godlieb et al. (2007a) (see Figure 6). Mixing times reduce with increasing operating pressure. This phenomenon is due to an increased number of bubbles, which yields more chaotic particle movement at elevated pressure, hence improving the mixing. A deviation from this trend is noticed at higher pressures (especially 64 bar). This can be explained by analysing snapshots of the particle positions (see Figures 7 and 8).

At a pressure of 64 bar, the bed tends to expand to almost twice the height at 2 bar. This has a large influence on mixing times, since the particles need to travel longer distances. The snapshots show that it takes more time for the bottom marker points to reach the top of the bed and hence, to fully mix.

To assess the mixing irrespective of the bed expansion, we also analysed the results for horizontal mixing. Since the horizontal pathway of the particles is bounded by the confining walls, bed expansion should have little effect on horizontal mixing. The results in Figure 5 (bottom)

confirm this idea: the horizontal mixing times decrease at high pressure.

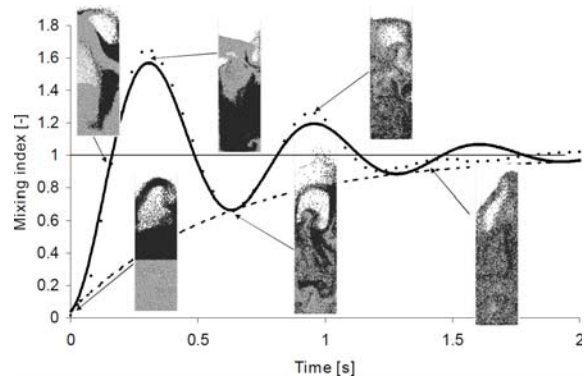


**Figure 4:** Mixing index versus time, resulting from simulations (o), a fit of the data using Eq. (25) (—), and Eq. (27) (- - -). Images of the particles present in a slice in the centre of the bed are shown as well.

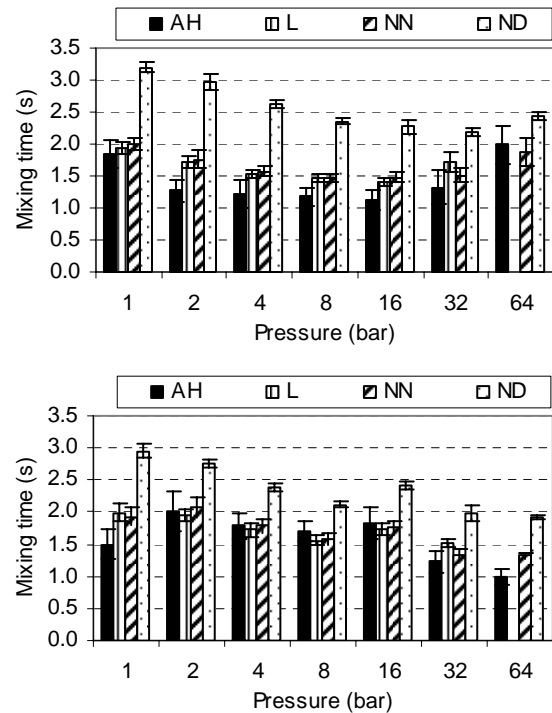


**Figure 5:** Mixing times versus operating pressure for vertical mixing (top) and horizontal mixing (bottom) from TFM simulation. AH is average height, L is Lacey, NN is nearest neighbours and ND is neighbour distance.

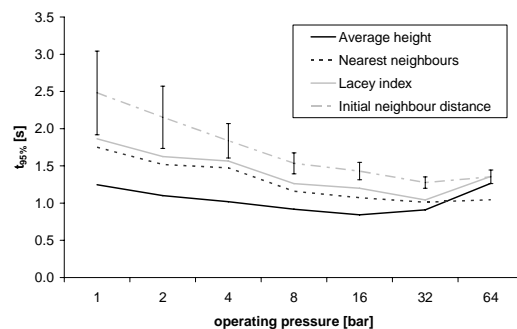


**Figure 6:** Mixing times vs. operating pressure for vertical mixing from DPM simulation (after Godlieb et al., 2007a).

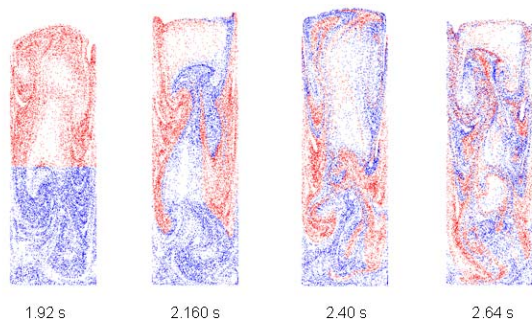


**Figure 7:** Snapshots of vertical mixing at 2 bar.

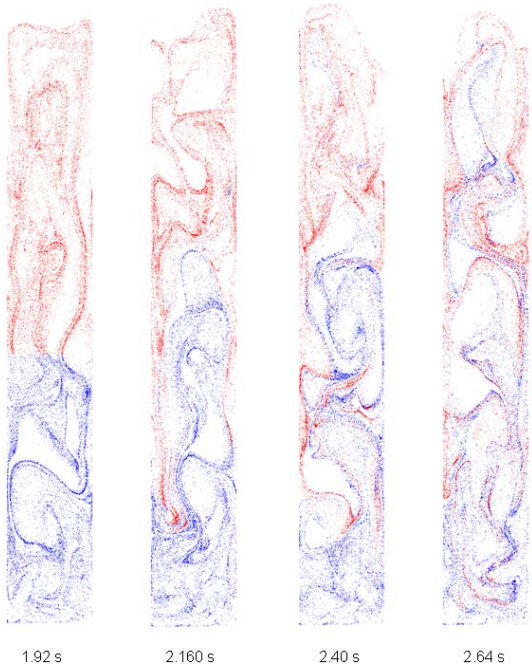


**Figure 8:** Snapshots of mixing at 64 bar.

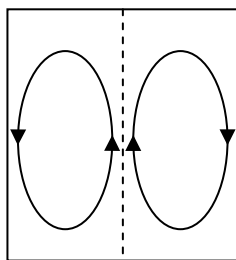


**Figure 9:** Schematic representation of average solids motion in a fluidized bed.

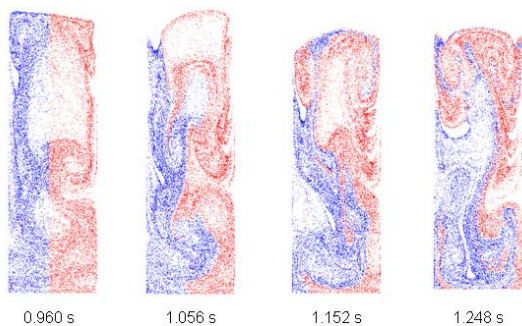


**Figure 10:** Horizontal mixing (1 bar).

For vertical mixing, increasing pressure has the effect that i) the number of bubbles increases and chaotic movement in the bed *enhances* (micro) mixing, and ii) the bed expansion increases the particle travelling distances and hence *decreases* (macro) mixing. The first effect is dominant in the range of 1-8 bars, whereas the second effect is most important at high pressures. However, the results of the horizontal mixing do not show a smooth trend of decreasing mixing time at low pressures. After studying particle position snapshots, it is concluded that bed expansion has an important effect on horizontal mixing after all, especially at lower pressures. This can be explained as follows. The average solids motion takes the form of two counter-rotating vortices (see Figure 9). Horizontal motion is only dominant in the top and the bottom zones of the bed. It is in these zones that the mixing of coloured particles starts (see Figure 10). Because mixing mostly happens at the top and bottom of the bed, the (expanded) bed height can influence horizontal mixing as well.

Extra simulations were performed to test the influence of bed height on the mixing times for vertical and horizontal mixing. For 2 and 32 bar, the initial bed height was reduced by 35%. Then again, mixing times were calculated. An average mixing time was determined by averaging the four mixing indices.

The results from these simulations are listed in Tables 1 and 2 and show that reducing the bed height has similar effects for 2 and 32 bar on the vertical mixing time. Both are reduced with ~11 %. For horizontal mixing however, results are different, i.e. the mixing time is less influenced than in vertical direction (only 6 % reduction) for 32 bar, but reduced significantly for 2 bar (16 %). This implies that i) horizontal mixing occurs partially via rotational movement of particles in the bed *decreasing* the mixing when a fluidized bed expands due to increasing pressure and ii) both direct horizontal motion and *increase* the mixing with increasing pressure, due to more chaotic movement in the bed and increasing space between the particles.

For high pressures, the second effect is dominant and therefore, horizontal mixing times are not so much affected by bed height as for lower pressures.

**Table 1:** Average vertical mixing times

p (bar)	$H_0$ (m)	Mixing time (s)	Normalized mixing time (-)
2	0.025	1.93	1.0
2	0.016	1.69	0.88
32	0.025	1.69	1.0
32	0.016	1.49	0.89

**Table 2:** Average horizontal mixing times

p (bar)	$H_0$ (m)	Mixing time (s)	Normalized mixing time (-)
2	0.025	2.21	1.0
2	0.016	1.85	0.84
32	0.025	1.52	1.0
32	0.016	1.43	0.94

## CONCLUSIONS

The average height method for analysing particle mixing can provide insight in overall mixing behaviour in a fluidized bed. Although, this method is very useful for visually monitoring mixing behaviour, it has the disadvantage that there is a restricted number of diversity (depending on the amount of different colours used) of the particles. To determine a mixing index, it is only important to know whether a particle has colour 1 or 2 and this restricts the first three methods in quantifying mixing behaviour. The neighbour distance method is the only method in which the mixing index does not depend on colouring, which makes it more suitable to quantify mixing.

The TFM simulations show useful trends and great similarity with the DPM simulations. The effects of increasing pressure on mixing behaviour are determined for vertical and horizontal mixing. For vertical mixing the following observations were made:

1. With increasing pressure, the number of bubbles increases, leading to more chaotic particle movement in the bed, which *enhances* vertical (micro) mixing;
2. Expansion of the bed increases particle travelling distances and *decreases* vertical (macro) mixing;

For increasing pressure, the second effect is dominant.

For horizontal mixing it was found that:

1. Horizontal mixing occurs partially via rotational movement of particles in the bed. Mixing *decreases* when a fluidized bed expands due to increasing pressure;
2. Direct horizontal motion and mixing of particles *increase* with increasing pressure, due to more chaotic movement in the bed and increasing space between the particles.

For increasing pressures, the latter is dominant and therefore horizontal mixing times are not so much affected by bed height as for lower pressures.

## ACKNOWLEDGEMENTS

This work is part of the Research Programme of the Dutch Polymer Institute (DPI) as project number #547.

## REFERENCES

ASMAR, B.N., LANGSTON, P.A., MATCHETT, A.J., (2002). A generalised mixing index in distinct element method simulation of vibrated particulate beds”, *Granular Matter*, **3**, 129-138.

BOKKERS, G.A., VAN SINT ANNALAND, M., KUIPERS, J.A.M., (2004). “Mixing and segregation in a bidisperse gas-solid fluidised bed: a numerical and experimental study”, *Powder Technol.*, **140**, 176-186.

DARELIUS, A., RASMUSON, A., VAN WACHEM, B., NIKLASSON BJØRN, I., FOLESTAD, S., (2008). “CFD simulation of the high shear mixing process using kinetic theory of granular flow and frictional stress models”, *Chem. Eng. Sci.*, **63**, 2188-2197.

FINNIE, G.J., KRUYT, N.P., YE, M., ZEILSTRA, C., KUIPERS, J.A.M., (2005). “Longitudinal and transverse mixing in rotary kilns: A discrete element method approach”, *Chem. Eng. Sci.*, **60**, 4083-4091.

GIDASPOW, D. (1994). “Multiphase flow and fluidization: Continuum and kinetic theory descriptions”, Boston, Academic Press.

GODLIEB, W., DEEN, N.G., KUIPERS, J.A.M., (2006). “Discrete particle simulations of high pressure fluidization”, *CHISA*, Prague, Czech Republic, paper 856.

GODLIEB, W., DEEN, N.G., KUIPERS, J.A.M., (2007a). “Characterizing solids mixing in DEM simulations”, *ICMF6*, Leipzig, Germany.

GODLIEB, W., DEEN, N.G., KUIPERS, J.A.M., (2007b). “A discrete particle simulation study of solids mixing in a pressurized fluidized bed”, *Fluidization XII*, Vancouver, Canada, 751-758.

GOLDSCHMIDT, M.J.V., KUIPERS, J.A.M. and VAN SWAAIJ, W.P.M., (2001). “Hydrodynamic modeling of dense gas-fluidised beds using the kinetic theory of granular flow: effect of coefficient of restitution on bed dynamics”, *Chem. Eng. Sci.*, **56**, 571-578.

HOOMANS, B.P.B., KUIPERS, J.A.M., BRIELS, W.J., VAN SWAAIJ, W.P.M., (1996). “Discrete particle simulation of bubble and slug formation in a two-dimensional gas-fluidised bed: A hard-sphere approach”, *Chem. Eng. Sci.*, **51**, 99-118.

HOOMANS, B.P.B., KUIPERS, J.A.M., VAN SWAAIJ, W.P.M., (2000). “Granular dynamics simulation of segregation phenomena in bubbling gas-fluidised beds”, *Powder Technol.*, **109**, 41-48.

KHARAZ, A.H., GORHAM, D.A., SALMAN, A.D., (1999). “Accurate measurement of particle impact parameters”, *Meas. Sci. Technol.*, **10**, 31.

LACEY, P., (1954). “Developments in theory of particulate mixing”, *J. Appl. Chem.*, **4**, 257.

Lu, L.-S., Hsiao, S.-S., (2005). “Mixing in vibrated granular beds with the effect of electrostatic force”, *Powder Technol.*, **160**, 170-179.

MCCARTHY, J.J., KHAKHAR, D.V., OTTINO, J.M., (2000). “Computational studies of granular mixing”, *Powder Technol.*, **109**, 72-82.

MOSTOUFI, N., CHAOUKI, J., (2001). “Local solid mixing in gas-solid fluidized beds”, *Powder Technol.*, **114**, 23-31.

RHODES, M.J., WANG, X.S., NGUYEN, M., STEWART, P., LIFFMAN, K., (2001). “Study of mixing in gas-fluidized beds using a DEM model”, *Chem. Eng. Sci.*, **56**, 2859-2866.

SCHUTYSER, M.A.I., PADDING, J.T., WEBER, F.J., BRIELS, W.J., RINZEMA, A., BOOM, R., (2001). “Discrete particle simulations predicting mixing behavior of solid substrate particles in a rotating drum fermenter”, *Biotechnol. Bioeng.*, **75**, 666-675.

VAN DER HOEF, M.A., BEETSTRA, R. and KUIPERS, J.A.M., (2005). “Lattice-Boltzmann simulations of low-Reynolds-number flow past mono- and bidisperse arrays of spheres: results for the permeability and drag force”, *J. Fluid Mech.*, **528**, 233-254

VAN DER HOEF, M.A., YE, M., VAN SINT ANNALAND, M., ANDREWS, A.T., SUNDARESAN, S., KUIPERS, J.A.M., GUY, B.M., (2006). “Multiscale modeling of gas-fluidized beds”, *Adv. Chem. Eng.*, **31**, 65-149.

VAN PUYVELDE, D.R., (2006). “Comparison of discrete elemental modelling to experimental data regarding mixing of solids in the transverse direction of a rotating kiln”, *Chem. Eng. Sci.*, **61**, 4462-4465.